

Quantum Hall-effect breakdown in silicon metal-insulator-semiconductor structures

Yu. V. Dubrovskii, M. S. Nunuparov, and M. I. Reznikov

Institute for Problems of Technology, Microelectronics, and Specially Pure Materials, USSR Academy of Sciences; Institute of Solid State Physics, USSR Academy of Sciences

(Submitted 12 August 1987)

Zh. Eksp. Teor. Fiz. **94**, 356–362 (March 1988)

An abrupt increase of σ_{xx} was observed in narrow Si(100) MIS structures with channel width 10 μm , under conditions of the quantum Hall effect (QHE) and with integer occupancy $i = 4$ of the Landau levels. As the electric field strength was increased, an S-shaped current-voltage characteristic and ensuing generation of sinusoidal voltage were observed in the inversion layer. The influence of the filamentation of the Hall current on the QHE breakdown in MIS structures is discussed. The experimental results are adequately described within the framework of the overheating-instability model.

INTRODUCTION

Breakdown of the quantum Hall effect (QHE), i.e., an abrupt increase of the diagonal component of the conductivity σ_{xx} or of the resistivity ρ_{xx} when the electric field strength or the current density reaches a critical value in a two-dimensional layer, has been the subject of many studies,^{1–11} in which at least five different breakdown mechanisms have been discussed. There is so far, however, no meeting of minds concerning the mechanism of the breakdown.

Most QHE breakdown experiments were performed on GaAs-Al_xGa_{1-x}As heterostructures,^{1–4} and in Refs. 1–3 was observed not merely a steep but a jumplike increase of ρ_{xx} when the Hall voltage U_H reached a certain critical value.

No jumplike dependence of ρ_{xx} on U_H was observed in the studies known to us of the QHE in MIS structures,^{5,6} which makes the determination of the breakdown voltage problematic. Moreover, as shown convincingly in Refs. 12 and 13, the current in MIS structures has under QHE conditions a highly inhomogeneous distribution, and this inhomogeneity leads to an exponential current-voltage characteristic¹³ in no way connected with the departure from Ohm's law, and hence with the QHE breakdown. This phenomenon was named filamentation of the Hall current.

For an experimental study of the breakdown one must attempt to obtain a uniform distribution of the current over the sample; this can be done by decreasing the sample width.

In observation of the QHE destruction one must track the variation of ρ_{xx} with the current in the Hall sample, or of σ_{xx} as a function of the drain-source voltage in a sample with Corbino geometry. Measurements of small values of ρ_{xx} of narrow samples is difficult in view of the small measurement currents. It is therefore more convenient to perform the experiment with Corbino-geometry samples.

SAMPLES AND MEASUREMENTS

We used Si(100) MIS structures with channel width 10 μm and below-gate oxide thickness 700 \AA thick, with the sample geometry close to that of a Corbino disk. The size and shape of the samples is shown in the inset of Fig. 1. The samples had polysilicon gates. The maximum electron mobility was $1.4 \cdot 10^4 \text{ cm}^2/\text{V}\cdot\text{s}$. To avoid hysteresis due apparently to the traps in the polysilicon, the samples were illuminated in the course of the measurements by an AL-103

red-light-emitting diode. The current through the sample was maintained constant, and the drain-source voltage was measured as a function of the voltage on the gate. Typical plots are shown in Fig. 1a. Plots of the current vs the maximum drain-source voltage U for a given current are shown in Fig. 2 for two samples under different conditions.

For one of the samples, with a bias—10 V applied to the substrate, the plot of the current against the drain-source voltage shows at 45 mV a current jump from $1 \cdot 10^{-7}$ to $6.5 \cdot 10^{-7}$ A. When plotted in the given-current regime, the current-voltage characteristic has in this current range a weakly pronounced S-shape. At currents from 1.5 to $6.5 \cdot 10^{-7}$ A an alternating signal was generated, having a frequency 10–100 kHz, an amplitude dependent on the gate voltage and current, the frequency being also dependent on the parameters of the external circuits. The alternating signal was displayed on an oscilloscope and its amplitude was recorded with a broadband amplifier. The fact that generation was observed confirms the presence of a section with negative differential resistance in the indicated current range. The amplitude of the alternating signal was a maximum at a current $4.5 \cdot 10^{-7}$ A through the sample. The de-

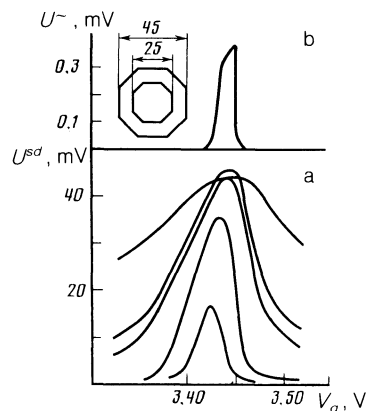


FIG. 1. Examples of experimental plots. Sample 2, substrate bias — 10 V. a) Drain-source voltage vs gate voltage. The curves (reading down) correspond to the currents I : $5 \cdot 10^{-11}$ A, $1 \cdot 10^{-9}$, $5 \cdot 10^{-8}$, $1 \cdot 10^{-7}$, $6.5 \cdot 10^{-7}$ A. The maximum on the curve corresponding to the current $I = 6.5 \cdot 10^{-7}$ A lies lower than that of the curve for $I = 1 \cdot 10^{-7}$ A, meaning an S-shaped current-voltage characteristic. b) Amplitude of generated sinusoidal signal vs the gate voltage at a current $4.5 \cdot 10^{-7}$ A. The inset shows the sample geometry. The dimensions are in microns.

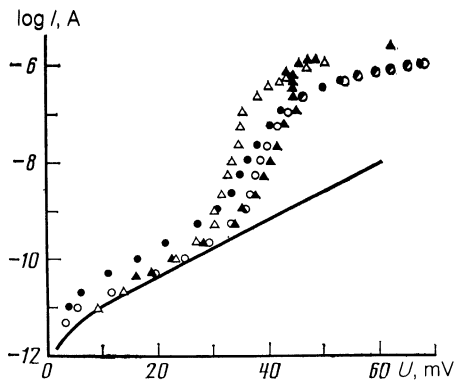


FIG. 2. Current through sample vs the maximum drain-source voltage for a given current. Magnetic field $B = 10$ T. \circ —sample 1, $T = 1.7$ K; \bullet —sample 1, $T = 2.1$ K; \triangle —sample 2, $T = 1.7$ K; \blacktriangle —sample 2, $T = 1.7$ K, substrate bias -10 V. Solid curve—plot obtained by fitting in accordance with Eq. (1).

pendence of the ac signal amplitude on the gate voltage is shown for this current in Fig. 1b.

DISCUSSION OF EXPERIMENTAL RESULTS

1. Influence of the filamentation on the current-voltage characteristic in the non-ohmic regime

The physical cause of filamentation in an MIS structure order QHE conditions is the extremely steep dependence of the diagonal component σ_{xx} on the electron density in the two-dimensional layer. The density depends in turn on the potential difference between the gate and the given point of the layer. Current flow causes a potential difference in the layer, while the density, and with it the conductivity, turns out to be a function of the coordinates, and it is this which leads to filamentation of the current.

An analytic calculation of the current flow in an MIS structure in the ohmic regime was carried out for a simple phenomenological model in Ref. 13. It was assumed that $\sigma_{xx} = \sigma_0 \exp(-\Delta/T) \cosh[(\varphi - V_0)/(2\nu T)]$, where $\nu = eD/c_0$, Δ is the activation energy, φ the potential at a given point of the layer relative to the gate, V_0 the layer-gate potential difference corresponding to an integer occupancy factor, D the density of states in the gap between the Landau levels, and c_0 the specific capacitance of the MIS structure.

For Corbino-geometry samples, the maximum U on the plot of the source-drain voltage U^{sd} vs the gate voltage is observed at $V_g^m = V_0 + U/2$. The current through the sample is then

$$I = \frac{4\pi\sigma_0 \exp(-\Delta/T)\nu T}{\ln(R_0/r_0)} \operatorname{sh} \frac{U}{2\nu T}, \quad (1)$$

where R_0 and r_0 are the outer and inner radii of the Corbino disk. The filamentation becomes substantial, and the current-voltage characteristic nonlinear, at $U \gtrsim 2\nu T$.

The solid curve of Fig. 2 is the current-voltage characteristic calculated from Eq. (1) for filamentation in the ohmic regime. The fit parameter νT was found to be 3.7 mV, corresponding to a density of states $D = 8 \cdot 10^{12} \text{ cm}^{-2}$ in the gap between the Landau levels.

This density of states agrees with the results of Ref. 14. It can be seen that the initial section of the experimental current-voltage characteristic can be wholly attributed to

ohmic filamentation. We attribute the abrupt increase of the current at $U \approx 25$ –45 mV, which leads to deviation from the solid curve of Fig. 2, to the onset of non-ohmic behavior in the sample. The sample-voltage range is $U > 2\nu T \sim 7.4$ mV, pointing to the presence of filamentation.

The abrupt current growth stops when the sample voltage becomes $\gtrsim 45$ mV. The dependence of U^{sd} on the gate voltage V_g becomes smooth (the curve corresponding to the current $6.5 \cdot 10^{-7}$ A in Fig. 1) in the gate-voltage range $V_g^m \pm U/2$, attesting to the absence of filamentation. The current and the electric field are then almost uniformly distributed. The electric field density in which the strong non-ohmic behavior ceases is $E_c \approx U/(R_0 - r_0) \sim 45 \text{ V} \cdot \text{cm}^{-1}$.

Let us estimate the voltage U at which the non-ohmic behavior sets in. We assume to this end that the conductivity increases jumpwise when the electric field reaches the value E_c . For a samples in a Corbino geometry, the dependence of the electric field on the radius r is given by

$$E(r) = I/2\pi r \sigma(r).$$

For $V_g = V_g^m$ the minimum value of $\sigma_{xx}(r)$ is $\sigma_0 e^{-\Delta/T}$ and is reached at a radius $r = R_0 r_0^{1/2}$. The intensity E reaches a critical value E_c at a current $I = 2\pi(R_0 r_0)^{1/2} \sigma_0 e^{-\Delta/T} E_c$. Substituting this current in (1), we obtain for the value of U at which non-ohmic behavior is expected to set in

$$U = 2\nu T \alpha, \quad \alpha = \operatorname{arcsch} \left[\frac{(R_0 r_0)^{1/2} \ln(R_0/r_0) E_c}{2\nu T} \right]. \quad (2)$$

In our experiment, $2R = 45 \mu\text{m}$ and $2r_0 = 25 \mu\text{m}$. At $\nu T = 3.7$ mV and $E_c = 45 \text{ V} \cdot \text{cm}^{-1}$ we get $\alpha = 3.2$, and non-ohmic behavior sets in at $U \approx 25$ mV. As seen from Fig. 2, this is a good estimate for the start of the deviation from ohmic filamentation.

With further increase of the drain-source voltage, the field intensity in the filament ceases to increase. The filament begins to expand, and the diagonal component of the conductivity in it increases. If the filament boundaries reach the sample boundaries before the conductivity in the latter exceeds the conductivity in the post-breakdown region, a current jump should accompany any further increase of U . In the opposite case, the current-voltage characteristic is smooth. Such a current jump is observed for sample 2 at a substrate bias -10 V when measured in a circuit with a specified drain-source voltage. For other samples, and also for sample 2 without a bias, we observed no current jump. It is not quite clear why the bias makes the breakdown more abrupt.

The following explanation, however, is possible. The bias on the substrate decreases the electron mobility.¹⁵ This should increase the density of states in the gap between the Landau levels and increase ν . The latter in turn decreases the influence of filamentation. The coefficient α is then decreased, and the sample becomes so to speak effectively narrower. Favoring this assumption is also the fact that the voltage U at which the deviation from ohmic filamentation sets in is larger for a biased than an unbiased sample, in full agreement with the estimate (2).

Expression (2) permits an analysis of the manifestation of the QHE breakdown in MIS structures of various widths. If the sample is narrow, such that $\alpha \ll 1$, the drain-source voltage will not change substantially the occupancy factor

on the edges of the sample following the breakdown. The field intensity in the sample will be uniform, and the breakdown will take place simultaneously over the entire sample. The current through the sample depends strongly on the drain-source voltage. For a broad sample, such that $\alpha \gg 1$, the main cause of the growth of the current through the sample with increase of the drain-source voltage is not breakdown in the current filament, but the increased conductivities of the regions outside the current filament, just as in the case of the ohmic regime.¹³ In this case the breakdown hardly influences the current-voltage characteristic. In samples of intermediate width, as in our experiments, the breakdown is smeared. It starts at the voltage given by Eq. (2) and ends at $U \sim E_c (R_0 - r_0)$.

We have thus observed a strong non-ohmic behavior in MIS structure under QHE conditions at an occupancy factor $i = 4$, in a magnetic field 10 T, and at a temperature 1.7 K. The electric field intensity at which this behavior sets in does not exceed 45 V/cm. One of the samples had an S-shaped current-voltage characteristic. Filamentation accounts for the more gently sloping current-voltage characteristics of other samples, as well as of the sample with the S-shaped current-voltage characteristic but at lower voltages. The QHE breakdown is expected to be more abrupt for narrower samples, as well as for samples with larger thickness of the insulator (with larger ν).

2. Breakdown mechanism in MIS structures

We discuss first the connection between our results and those of Refs. 5 and 6, in which QHE breakdown in MIS structures was investigated. In both cited papers the measured Hall samples were broad, and no jumplike growth of the current was observed in them with increase of the Hall voltage. These results can apparently be satisfactorily attributed to filamentation within the framework of the model discussed in detail above.

Note that the authors of Ref. 6, having observed that the "critical current density" in short broad samples is much lower than in narrow long ones, have attributed this result to emission of hot carriers from the near-contact regions, where a strong electric field is present.¹⁶ The "critical current density," however, was determined assuming a uniform current distribution over the sample, which is utterly untrue under filamentation conditions. There is therefore no need to invoke emission from the contact regions to explain the results of Ref. 6. Moreover, if emission from the contact region is assumed, the QHE destruction near the drain and the source should occur earlier than at the center of the sample. We have verified this assumption, using a Hall sample with potential contacts at various distances from the drain and source. The measured current-voltage characteristics, corrected for a geometric factor, turned out to be practically identical. This mechanism is impossible in principle in Corbino-geometry samples.

In our opinion, the available set of experimental data can be satisfactorily explained only as being due to heating of the electron system.^{1,2,4} Assume that the conductivity depends only on the electron energy distribution and is independent of the lattice temperature,¹ and that the frequency of the electron-electron collisions is high enough to be able to describe the electron distribution function by a temperature T_E (the validity of both assumptions is far from obvious).

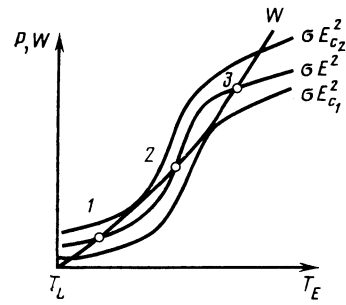


FIG. 3. Power W transferred from the electron system to the lattice, and power P received by the electron system from the electric field, vs the electron temperature; the parameter is the electric field. In the field range $E_{c_1} < E < E_{c_2}$, the plots of W and P intersect at three points, with points 1 and 3 stable. The figure illustrates the onset of the overheating instability.

We plot, following Gurevich and Mints¹⁷ (see Fig. 3), the power P absorbed by the electron system from the electric field, and the power W drawn from the electrons by the lattice, as functions of the electron temperature. If W does not increase too rapidly with rise of the electron temperature, the $P(T_E)$ and $W(T_E)$ plots intersect in the electric-field range $E_{c_1} < E < E_{c_2}$ at three points. Points 1 and 3 are stable states of the system, the current-voltage characteristic is found to be S-shaped. The QHE breakdown should occur when the electric field reaches the value E_{c_1} . We assume that it is just this mechanism which is responsible for S-shaped plot observed by us for biased sample 1 and for the ensuing generation.

To explain the QHE breakdown observed in heterostructures, an attempt was made in Ref. 4. to obtain quantitative $\sigma(E)$ plots by solving the energy-balance equation $P(T_E \equiv \sigma_{xx}(T_E) E^2 = W(T_E))$. As a result of the calculations, the authors obtained an S-shaped current-voltage characteristic, and the calculated curves were very similar to the experimental ones (although no S-shaped characteristic was observed in Ref. 4). It seems, however, that the assumptions made in Ref. 4 for the calculation of the $W(T_E)$ dependence are not sufficiently well founded, especially the approximation used for the energy relaxation time $\tau(T_E, T_L)$ (T_L is the lattice temperature). The point is that to estimate $\tau(T_E, T_L)$ the authors used the results of Ref. 18, obtained under the assumption that the Landau-level broadening is due to electron-phonon scattering, whereas it is actually due to elastic interactions with impurities. The calculation results, however, are not too sensitive to the stipulated $W(T_E, T_L)$ dependence.

There is at present no calculation of $\tau(T_E, T_L)$ for a two-dimensional system in a strong magnetic field, with allowance for impurities. Simulation of the experimental curve is therefore impossible. Since current filamentation takes place in the pre-breakdown voltage region, it is impossible to determine from Fig. 2 the conductivity $\sigma_{xx}(E)$ and to calculate the energy-relaxation time. At sample voltages above breakdown, no filamentation takes place, so that the conductivity $\sigma(E)$ can be determined. Using the conductivity temperature dependence plotted in the linear regime we can determine under the foregoing assumptions the electron temperature and estimate the energy-relaxation time from the energy-balance equation $W(T_E, T_L) = P(E)$:

$$W(T_E, T_L) = \frac{\varepsilon(T_E) - \varepsilon(T_L)}{\tau(T_E, T_L)}, \quad P(E) = \sigma_{xx}(T_E) E^2, \quad (3)$$

where $\varepsilon(T)$ is the electron-system temperature.

At sufficiently high temperatures (the electron-gas temperature after breakdown, determined from the conductivity, is ≈ 5.4 K), the specific heat of the electron gas is determined by the transfer from the occupied Landau level to the empty one.¹⁹ In this case $\varepsilon(T) = N_s \hbar\omega / [\exp(\hbar\omega/2T) + 1]$, where N_s is the number of electrons on the Landau level (with allowance for degeneracy). The value of τ estimated in this manner is $3 \cdot 10^{-10}$ s, in reasonable agreement with the results of Refs. 4 and 20.

To explain the QHE breakdown we can invoke, besides injection of hot electrons from the contact region and superheat instability, three other mechanisms:

*Zener tunneling between Landau levels.*⁷ This mechanism requires an electric field strong enough to produce a change $\sim \hbar\omega_c$ in the potential of the layer over a distance on the order of the magnetic length. The experimentally observed breakdown field is lower by at least two orders of magnitude.

*Acoustic-phonon emission when the carrier drift velocity reaches that of sound.*⁸⁻¹⁰ The Hall current density in a field of intensity 45 V/cm at an occupancy factor $i=4$ is $6.8 \cdot 10^{-3}$ A·cm⁻¹. The average carrier drift velocity is then $v_d = 4.3 \cdot 10^4$ cm·s⁻¹, much lower than the speed of sound $v_s = 8.4 \cdot 10^5$ cm·s⁻¹ in silicon.²¹ This difference is at variance with the model proposed in Refs. 8-10. Note that in heterostructures, at a breakdown v_d is less than v_s by only approximately a factor of two, so that this mechanism could not be unequivocally rejected.^{2,3}

As to the *increase of the number of extended states with increase of the electric field strength*,¹¹ we cannot compare our results with the predictions of the theory for lack of quantitative estimates.

In our opinion, the electric field strengths in which QHE breakdown, S-shaped current-voltage characteristics, and reasonable estimates of the energy-relaxation time take place show that the QHE breakdown is due to superheating of the electronic system.

The authors thank V. A. Grazhulis, S. I. Dorozhkin, I. B. Levinson, and V. I. Tal'yanskiĭ for most helpful discussions.

¹G. Ebert, K. von Klitzing, and G. Weimann, *J. Phys.* **C16**, 5441 (1983).

²M. E. Cage, R. F. Dziuba, B. F. Field, *et al.*, *Phys. Rev. Lett.* **51**, 1374 (1983).

³H. L. Störmer, A. M. Chang, D. C. Tsui, and J. C. M. Hwang, *Proc. 17th Intern. Conf. Phys. Semicond.*, San Francisco, Springer, 1984, p. 267.

⁴S. Komiyama, T. Takamasu, S. Hiyamizu, and S. Sasa, *Sol. St. Comm.* **54**, 479 (1985).

⁵K. von Klitzing, G. Ebert, N. Kleinmichel *et al.*, *Ref. 3*, p. 271.

⁶K. Voshihiro, J. Kinoshita, K. Inasaki, *et al.*, *Surf. Sci.* **170**, 193 (1986).

⁷D. C. Tsui, G. J. Dolan, and A. C. Gossard, *Bull. Amer. Phys. Soc.* **28**, 365 (1983).

⁸P. Streda and K. von Klitzing, *J. Phys.* **C17**, 483 (1984).

⁹O. Heinonen, P. L. Taylor, and S. M. Girvin, *Phys. Rev.* **B30**, 3016 (1984).

¹⁰P. Streda, *J. Phys.* **C19**, 2155 (1986).

¹¹S. A. Trugman, *Phys. Rev.* **B27**, 7539 (1983).

¹²V. M. Pudalov and S. G. Semenchinskiĭ, *Pis'ma Zh. Eksp. Teor. Fiz.* **42**, 188 (1985) [*JETP Lett.* **42**, 232 (1985)].

¹³A. A. Shashkin, V. T. Dolgoplov, and S. I. Dorozhkin, *Zh. Eksp. Teor. Phys.* **91**, 1897 (1986) [*Sov. Phys. JETP* **64**, 1124 (1986)].

¹⁴V. T. Dolgoplov, S. I. Dorozhkin, and A. A. Shashkin, *ibid.* **92**, 1782 (1987) [**65**, 999 (1987)].

¹⁵A. Hartstein, A. B. Fowler, and M. Albert, *Surf. Sci.* **98**, 181 (1980).

¹⁶N. A. Usov and F. R. Ulinich, *Pis'ma Zh. Eksp. Teor. Fiz.* **40**, 306 (1984) [*JETP Lett.* **40**, 1096 (1984)].

¹⁷A. V. Gurevich and R. G. Mints, *ibid.* **39**, 318 (1984) [**39**, 381 (1984)].

¹⁸M. Prasad and M. Singh, *Phys. Rev.* **B29**, 4803 (1984).

¹⁹W. Zawadzki and R. Lassnig, *Surf. Sci.* **142**, 225 (1984).

²⁰H. Sakaki, T. Hirokava, J. Yosino, *et al.*, *ibid.* **142**, 306 (1984).

²¹American Institute of Physics Handbook, 3rd ed., D. E. Gray *et al.*, eds., McGraw, 1972.

Translated by J. G. Adashko